Single-Molecular-System-Based Selective Micellar Templates for Polyaniline Nanomaterials: Control of Shape, Size, Solid State Ordering, and Expanded Chain to Coillike Conformation

ARTICLE *in* MACROMOLECULES · AUGUST 2007

Impact Factor: 5.8 · DOI: 10.1021/ma071292s

2 AUTHORS:

Anilkumar Parambath
University of British Columbia - Vancouver
28 PUBLICATIONS **793** CITATIONS
SEE PROFILE

Manickam Jayakannan
Indian Institute of Science Education and Re…
74 PUBLICATIONS **1,566** CITATIONS
SEE PROFILE

Single-Molecular-System-Based Selective Micellar Templates for Polyaniline Nanomaterials: Control of Shape, Size, Solid State Ordering, and Expanded Chain to Coillike Conformation

P. Anilkumar and M. Jayakannan*

Polymer Research Group, Chemical Sciences & Technology Division, National Institute for Interdisciplinary Science and Technology (Formerly: Regional Research Laboratory), Thiruvananthapuram 695019, Kerala, India

Received June 11, 2007; Revised Manuscript Received July 13, 2007

ABSTRACT: A single molecular approach has been developed to selectively template polyaniline nanomaterials via interfacial and emulsion polymerization routes to control the nanomaterials shape, size, solubility, solid state ordering, and expanded polymer chain to coil-like conformation. A new amphiphilic azobenzenesulfonic acid dopant was designed and developed from renewable resource cardanol which exists in the form of 4.3 nm spherical micelles in water. The amphiphilic micelles selectively undergo spherical or cylindrical aggregation with ammonium persulfate (APS) and aniline in water at ambient conditions. In the interfacial route, aniline molecules diffuse through the interface and get oxidized by the dopant−APS spherical pre-aggregates to produce polyaniline nanospheres of 400 nm in diameter. The oxidations of dopant-aniline cylindrical micelles by APS in the emulsion route produce polyaniline nanofibers of 150−200 nm diameters with length up to 5−8 μM. The mechanistic aspects of the polyaniline nanomaterials formation was investigated by dynamic light scattering to trace the factors which control the morphology of the resultant materials. The aniline/dopant ratio was varied from 100 to 450 to study the effect of reactants composition on the morphology and mechanism of the nanomaterials formation. The presence of hydrophobic tail in the amphiphilic dopant increases the solubility of nanospheres and nanofibers in water as well as organic solvents such as chloroform, *n*-butanol, chlorobenzene, xylene, and *m*-cresol, etc. The absorbance spectra of the nanospheres showed a free carrier tail above 950 nm in the near IR region for the delocalization of electrons in the polaron band corresponding to expanded conformation of polyaniline chains whereas the polyaniline nanofibers showed a peak characteristics at 750−850 nm with respect to more coiled-like conformation. The solvent dependent absorption studies revealed that the conformations of the polymer nanomaterials are less influenced by the solvent in which they were suspended. WXRD patterns of nanofibers showed a peak at $2\theta = 6.4°$ (*d*-spacing = 13.6 Å) for polyaniline chain due to the effective inter-digitations of dopant molecules in the polyaniline crystalline domain. The expanded conformation of polymer chains enhances the solid state ordering of the nanospheres and a new intense peak at $2\theta = 6.05°$ (*d*-spacing 14.3 Å) is observed, which is absent in the case of nanofibers.

Introduction

Nanostructured polyaniline materials have attained wide interest for new applications in chemical[1−6] and biological sensors,[7−9] energy conversion and storage devices,[10] and microelectronics[11−13] etc. Approaches such as "hard and soft" templates,[14−19] interfacial,[20−23] rapid mixing,[24] electrochemical,[13,25] seeding,[10] oligomer assisted,[26] and dilute polymerization techniques[27] have been reported for the development of one and three (1D and 3D) dimensional polyaniline nanomaterials. Among these approaches, emulsion and interfacial polymerization techniques have attracted considerable interest owing to the simple procedures and also formation of high purity nanomaterials.[23] In the emulsion polymerization technique, the dopant acts as emulsifier for aniline in water to form micelles in water to produce nanostructured polyaniline materials. The synthesis of polyaniline nanofibers in the emulsion route was found highly susceptible to the dopant/aniline ratio in the feed and good homogeneous nanofibers were produced only for selective compositions.[28] The reason for the inhomogeneity in the nanofiber formation was rationalized to the poor micelles formation in water, and it was understood that the structural design of the sulfonic acid is crucial in the stabilization of micelles for the successful growth of polyaniline nanofibers.[28,29] External surfactants such as alkyltrimethylammonium bromide or sodium dodecylbenzenesulfonate were utilized to form emulsion template for assisting dopants such as inorganic mineral acids and sulfonic acids.[30−32] However, the removal of these surfactant molecules during the purification step significantly influence on the properties of the end nanomaterials such as solubility, conductivity and processability. Kaner and co-workers developed an interfacial polymerization route for polyaniline nanofibers[20,21] and in this route the polymerization is performed in an immiscible aqueous/organic two-phase system. The polymerization occurs at the interface and the resultant polyaniline in its hydrophilic emeraldine salt form diffuses away from the reactive interface which makes more reaction sites available at the interface.[21] The interfacial route is mostly restricted to <1 g scale (also low yield) due to the difficulty in controlling the diffusion process at the interfaces for large scale synthesis of polyaniline nanomaterials.[20] Interestingly, the nanofibers produced through interfacial route were thin (<100 nm), free from agglomerates and easily dispersible in water compared to other synthetic routes.[21] The idea of utilizing a single molecular dopant system in both emulsion and interfacial routes to trace the factors which control the morphology of the nanomaterials is crucial and important for fundamental understanding of polyaniline nanomaterials. However,

* Corresponding author. E-mail: jayakannan18@yahoo.co.in, Fax: 0091-471-2491712.

10.1021/ma071292s CCC: $37.00
Published on Web 08/29/2007

the efforts to investigate these two well-known polymerization routes in a single dopant system is not explored because of the poor micellar formation by interfacial-loving dopants (freely soluble in water) in the emulsion route and vice versa.

Recently we have reported a renewable resource strategy for polyaniline nanomaterials based on a raw material, cardanol, which is an industrial waste and pollutant from the cashew nut industry.[33,34] A new amphiphilic molecule, 4-[4-hydroxy-2-((*Z*)-pentadec-8-enyl)phenylazo]benzenesulfonic acid, was developed from cardanol and employed as a dopant to produce polyaniline microspheres, dendritic nanofibers, linear nanofibers, and nanotubes via self-assembly approach.[33,34] The amphiphilic molecule has an inbuilt head to tail geometry to form stable micelles of 4.3 nm diameters in water and potential dual amphiphilic sulfonic acid derivative for emulsion and interfacial routes. Here, the unique amphiphilic character of the dopant molecule was utilized to selectively template the interfacial and emulsion routes (a single molecular approach) to tune the size, shape, solid state ordering and expanded chain to coil-like conformation of polyaniline nanomaterials. Dynamic light scattering (DLS) experiments were performed for the polymerization mixtures to trace the templating behavior of the dopant molecule. DLS studies revealed that the dopant micelles form selectively spherical or cylindrical aggregates with ammonium persulfate or aniline in water, respectively. The spherical aggregates induce the formation of nanospheres (interfacial route) whereas the cylindrical aggregates lead to the formation of nanofibers (emulsion route). The morphologies of the nanomaterials were characterized by SEM and TEM and the size distribution of the spheres were determined by particle size analyzer. The absorption spectroscopy and X-ray diffraction studies revealed that the nanospheres produced by the interfacial route is highly ordered with expanded chain conformation compared to the nanofibers produced by the same dopant via emulsion route. The amphiphilic nature of dopant enhances the solubility of the nanospheres (also fibers) and they can be dispersed in various solvents like water, alcohol, chloroform, chlorobenzene, *m*-cresol, and xylene etc.

Experimental Section

Materials. Aniline, ammonium per sulfate (APS), sulfanilic acid, hydrochloric acid, and sodium hydroxide were purchased locally and purified. Cardanol was purified by double vacuum distillation at 3−4 mm of Hg and the fraction distilled at 220−235 °C was collected.[35] The dopant molecule was synthesized by following the reported procedures and purified by silica gel column chromatography.[33,34]

Measurements. For SEM measurements, polymer samples were subjected for thin gold coating using JEOL JFC-1200 fine coater. The probing side was inserted into JEOL JSM-5600 LV scanning electron microscope for taking photographs. Transmission electron microscope images were recorded using a Hitachi H-600 instrument at 75 kV. For TEM measurements, the water suspension of nanomaterials were prepared under ultrasonic and deposited on Formvar coated copper grid. Wide-angle X-ray diffractions of the finely powdered polymer samples were recorded by Philips Analytical diffractometer using Cu K-alpha emission. For dynamic light scattering (DLS) measurements, we used a Nano ZS Malvern instrument employing a 4 mW He−Ne laser ($\lambda = 632.8$ nm) and equipped with a thermo stated sample chamber. Particle size distributions of nanospheres were measured using laser light scattering method using Malvern Zeta Sizer instruments. Infrared spectra of the polymers were recorded using a Perkin-Elmer, spectrum one FTIR spectrophotometer in the range 4000−400 cm^{-1}. For conductivity measurements, the polymer samples were pressed into a 10 mm diameter disk and analyzed using a four probe conductivity instrument by applying a constant current. The resistivity of the samples was measured at five different positions and at least two pellets were measured for each sample: the average of 10 readings was used for conductivity calculations. The thermal stability of the polymers was determined using TGA-50 Shimadzu thermogravimetric analyzer at a heating rate of 10 °C/min in nitrogen. Uv-vis spectra of the PANI in water were recorded using Perkin-Elmer Lambda-35 UV−vis spectrophotometer.

Interfacial Route for Polyaniline Nanomaterials. The synthesis of polyaniline is described in detail for **P-I-100** and other two samples were prepared following the same procedure. The dopant **1** (0.053 g, 0.11 mmol) and ammonium persulfate (2.5 g, 11.00 mmol) were dissolved in doubly distilled water (30 mL) in a 50 mL glass vial. In a separate glass vial distilled aniline (1 mL, 1.02 g, 11.00 mmol aniline/dopant = 100) was dissolved in dichloromethane. To the dichloromethane solution, dopant plus oxidant in water was carefully added without disturbing the interface. The interfacial polymerization was allowed to stand at 30 °C for 15 h without disturbing. Then the polyaniline solid mass was formed in the aqueous phase which was centrifuged, washed with distilled water and methanol for several times until the filtrate become colorless. The solid product was dried in a vacuum oven at 60 °C for 48 h (0.01 mmHg). Yield = 0.36 g (35%). FT-IR (in cm^{-1}): 3015.8, 1563.5, 1484.3, 1301.2, 1248.8, 1151.4, 1106.3, 1027.9, 812.7, 707.4, and 618.4.

Emulsion Route for Polyaniline Nanomaterials. Typical procedure for the synthesis of polyaniline nanofiber is described in detail for **P-E-100** and other two samples were prepared following the same procedure. The dopant **1** (0.053 g,0.11 mmol) was dissolved in doubly distilled water (20 mL) and stirred under ultrasonic for 1 h at 30 °C. Distilled aniline (1 mL, 1.02 g, 11.00 mmol, aniline/dopant = 100) was added to the dopant solution and stirred under ultrasonic for additional 1 h at 30 °C. At the end of the stirring, the formation of pale yellow emulsion was noticed. Ammonium per sulfate (1.1 M solution) was added at 5 °C and stirred under ultrasonic for 1 h at 5 °C. The resultant green color content was allowed to stand at 5 °C for 15 h without disturbing in a refrigerator. The solid mass was filtered, washed with distilled water, methanol and diethyl ether for several times until the filtrate become colorless. The solid product was dried in a vacuum oven at 60 °C for 48 h (0.01 mm of Hg). Yield = 0.80 g (76%). FT-IR (in cm^{-1}): 3010.8, 1579.7, 1500.6, 1305.8, 1224.8, 1159.2, 1031.9, 825, 705.9, and 628.7.

P-I-300, **P-I-450**, **P-E-300**, and **P-E-450** were prepared by varying aniline/dopant ratio as 300 and 450 mol by following the above procedure. The composition, yield, elemental analysis data (*S*/*N* ratio) were summarized in Table 1.

Results and Discussion

The amphiphilic dopant molecule, 4-[4-hydroxy-2-((*Z*)-pentadec-8-enyl)phenylazo]benzenesulfonic acid (dopant **1**, see Figure 1) was synthesized from renewable resource cardanol as reported earlier.[33,34] The dopant **1** has unique built-in amphiphilic design consisting of hydrophilic sulfonic acid as polar head and long alkyl chain as hydrophobic tail and forms micelles in water at ambient conditions. The polyaniline nanomaterials were prepared by two different polymerization approaches namely, interfacial polymerization and emulsion polymerization method. Interfacial polymerization is performed in an aqueous/organic two phase system with aniline dissolved in dichloromethane as solvent and ammonium peroxydisulfate + dopant were dissolved in an aqueous solution. The polyaniline samples were prepared by varying the aniline/dopant ratio in the feed as 100, 300, and 450 (in moles), respectively. The polymer were denoted as **P-I-*X*** (**P-I-100**, **P-I-300**, and **P-I-450**), where **I** and ***X*** refer to the interfacial route and ratio of aniline/dopant in the feed, respectively. Ammonium per sulfate and dopant-1 were dissolved in water and immediately transferred to a vial containing aniline in dichloromethane. It is

Table 1. Composition of Aniline/dopant, Conductivity, Dimensions and WXRD Data of Polyaniline Nanomaterials

						peaks in WXRD[g]	
sample[a]	aniline/dopant[b] (mol)	yield[c] (%)	S/N[d] (%)	σ[e] (S/cm)	diameter[f] (nm)	peak at 2θ (deg)	d-spacing (Å)
P-I-100	100	34	33.3	2.6×10^{-2}	sphere 400 nm−2.1 μm	6.1, 6.4, 18.3, 20.2, 25.6	14.46, 13.61, 4.83, 4.39, 3.46
P-I-300	300	36	31.3	5.2×10^{-2}	sphere 300−400 nm	6.1, 6.4, 18.2, 20.1, 25.3	14.59, 13.65, 4.87, 4.42, 3.51
P-I-450	450	41	32.4	1.6×10^{-2}	sphere + fiber 50−120 nm	6.4, 20.1, 25.4	13.66, 4.41, 3.49
P-E-100	100	71	31.6	7.5×10^{-3}	fiber 150−200 nm	6.4, 20.1, 25.6	13.7, 4.4, 3.5
P-E-300	300	75	29.9	9.5×10^{-3}	fiber 180−250 nm	6.5, 18.5, 25.6	13.54, 4.78, 3.47
P-E-450	450	81	29.7	3.0×10^{-3}	fiber 175−225 nm	6.5, 18.4, 25.9	13.54, 4.81, 3.43

[a] The symbols "I" and "E" refer to the fact that the samples were prepared via interfacial and emulsion polymerization routes [b] The concentration of aniline is fixed at 3.6 M^{-1}, and the amount of dopant is varied in water. [c] Calculated for isolated product [d] Determined from elemental analysis [e] Measured using four probe conductivity set up at 30 °C. [f] Average diameter is calculated based on SEM images. [g] Wide-angle X-ray diffraction measurements were carried out at 30 °C.

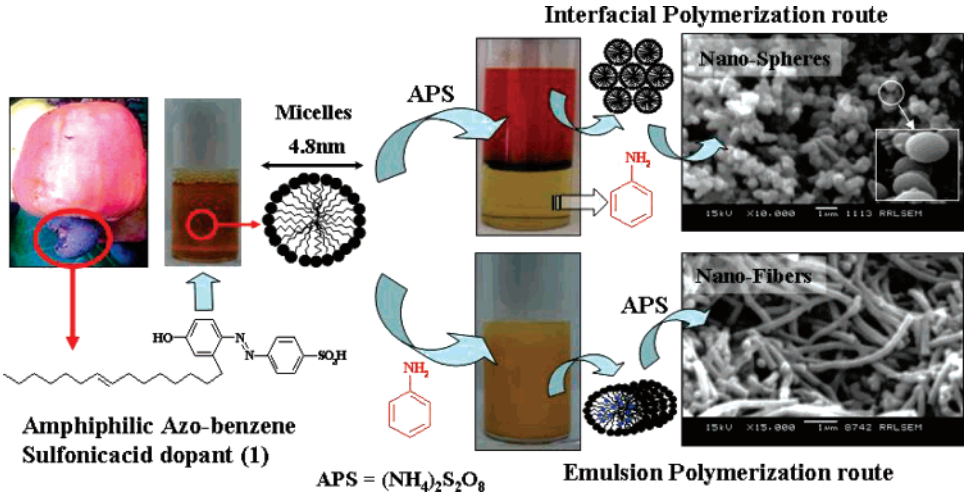

Figure 1. Synthesis of polyaniline nanomaterials using a renewable resource amphiphilic azobenzenesulfonic acid as a dopant.

observed (with in 2 min) that upon adding APS solution, the aqueous dopant layer slowly transform from clear yellow to turbid (see vials in Figure 1). After an induction period of 10 min, the polymerization started and green layer of polyaniline emeraldine appears at the interface (see vials in Supporting Information). As the reaction proceeds, the green layer became thick and after 15 h the entire aqueous layer turned to a dark solid. The aqueous layer was separated carefully, centrifuged and washed well with water and methanol to remove all oligomers, excess dopant and inorganic impurities. The polyaniline samples **P-E-*X*** (**P-E-100, P-E-300**, and **P-E-450,** where **E** for emulsion route and ***X*** for the aniline/dopant ratio in the feed) were prepared by emulsion polymerization technique. The polyaniline samples **P-E-100, P-E-300** and **P-E-450** were prepared by varying the aniline/dopant ratio in the feed as 100, 300, and 450 (the same as that of interfacial route), respectively. We have chosen the aniline/dopant ratio as 100 to 450 for the present investigation based on our previous studies that the dopant-aniline complex formed stable micelles in water at this composition range[34] (see vials in Supporting Information). The dopant **1** is freely soluble in water and its complex with aniline form stable emulsion, which acts as self-assisted template for polyaniline nanomaterials (see vial in figure-1). Typically the polymerization was carried out by dissolving aniline and dopant in water and subsequently stirring under ultrasonic at ambient conditions for 30 min. The resultant milky emulsion was oxidized by adding ammonium perdisulfate (1.1 M solution) in water and stirred at 0−5 °C under ultrasound for 1 h. The green solution was kept at 5 °C without disturbing in the refrigerator for 15 h. The green polymer was filtered and purified by washing with water and methanol until the filtrate become colorless. Both **P-I-*X*** and **P-E-*X*** samples were dried under vacuum for 24 h (0.05 mm of Hg) at 60 °C prior to further analysis. The yield, composition and elemental analysis data (S/N ratio) of the polyaniline nanomaterials are summarized in Table 1. The emulsion route samples were obtained in a good yield of about 70% whereas the interfacial route were in 40% yield, which is relatively much higher than that reported for other sulfonic acid dopants (for example camphorsulfonic acid, 8% yield).[20] The doping of the polyaniline nanomaterials was confirmed by FT-IR spectroscopy (see Supporting Information), elemental analysis (S/N ratio), UV−vis spectroscopy, and four-probe conductivity (see Table 1).

The morphologies of the polyaniline samples were recorded using a JEOL JSM-5600 LV scanning electron microscope, and SEM images of the polyaniline nanomaterials are given in Figures 2 and 3. The SEM images of interfacial samples showed an interesting observation that the morphology of the materials changing from microspheres to nanospheres plus fibers with the decreasing the amount of dopant in the feed (from aniline/dopant = 100 to 450 in moles). **P-I-100** consists of both micro- and nanospheres whereas **P-I-300** predominately has only nanospheres of ~ 400 nm diameter. The sample **P-I-450** has nanospheres (400 nm) and also thin nanofibers of <150 nm diameter. The SEM images of the emulsion route samples were completely different from that of the interfacial route. All three samples**, P-E-100**, **P-E-300**, and **P-E-450** have shown long polyaniline nanofibers of average diameter of ~200 nm with a length up to 8 μM (see Figure 3). SEM technique is inadequate to distinguish whether the nanomaterials are hollow or rigid and also poor resolution for <150 nm size (see Figure 2c).[28] Therefore, the polyaniline nanomaterial samples were subjected to TEM analysis and the TEM images of **P-I-300**, **P-I-450**, and **P-E-300** are given in Figure 4. TEM image of **P-I-300** appeared

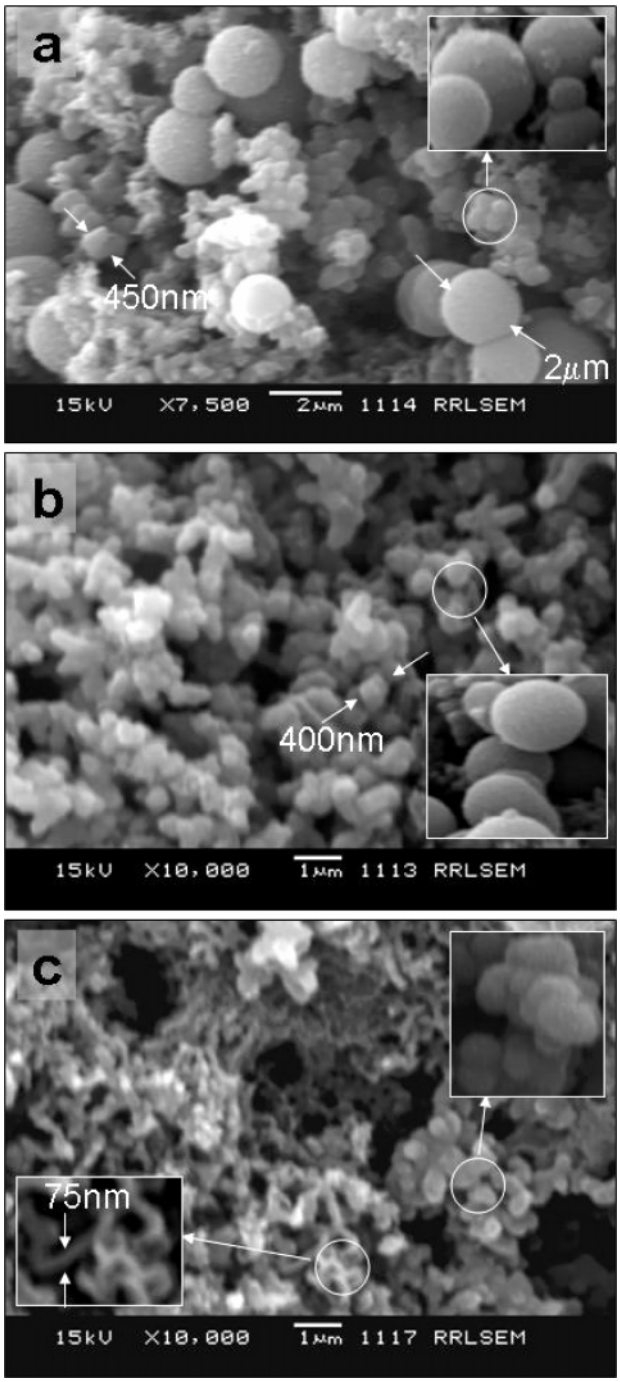

Figure 2. SEM images of polyaniline nanomaterials: (a) **P-I-100**, (b) **P-I-300**, and (c) **P-I-450**.

as a cluster of solid nanospheres with diameter 300 nm. In **P-I-450** the presence mixtures of thin nanofibers with nanospheres were clearly visible. The sample **P-E-300** contains only nanofibers with ~5 μM length and 200 nm in diameter, and there are no traces of nanospheres or nanotubes. The charged conducting nanomaterials have very strong affinities to each other and cluster together during the sample preparation (for TEM analysis) via solvent evaporation method. This leads to the TEM images of the nanospheres that look like a meso-structure, and a similar observation was also reported by other researchers.[38] It is clear from the morphological analysis by SEM and TEM that the polyaniline nanomaterials prepared by interfacial method are predominantly nanospheres and the emulsion method yields only nanofibers. In general, polyaniline nanofibers are commonly reported for interfacial route (for HCl and CSA);[20,21]

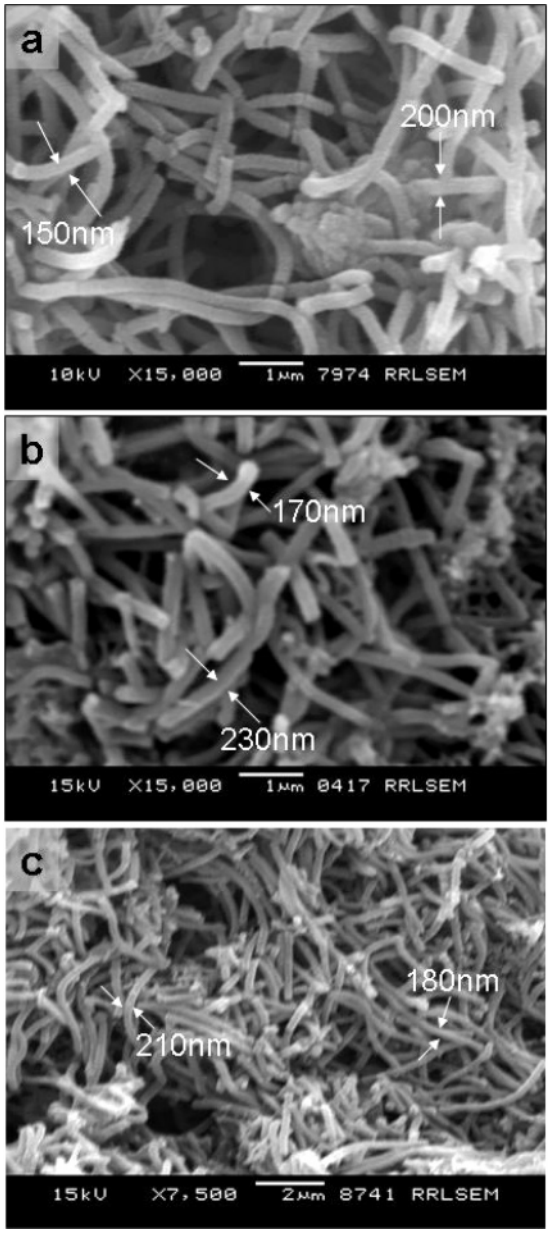

Figure 3. SEM images of polyaniline nanomaterials: (a) **P-E-100**, (b) **P-E-300**, and (c) **P-E-450**.

interestingly, for the first time we observed the formation of nanospheres. This suggests that the mechanism of formation of nanomaterials in interfacial route for the amphiphilic azobenzene dopant is different compared to other dopants reported so far. Additionally, the formations of different morphologies in the interfacial and emulsion routes (spheres and fibers) also indicate that the same dopant molecule follows different mechanistic pathways in both polymerization routes.

The dynamic light scattering (DLS) technique is an efficient tool that may be used to study the micellar behavior of aniline with dopant molecules in water.[36,37] DLS measurements were carried out for dopant alone and also two types of complexes: (i) aniline + dopant and (ii) APS + dopant to trace factors which influence the morphology of the nanomaterials in the interfacial and emulsion routes. DLS data for the dopant alone and above two complexes are given in Figure 5. DLS data for the dopant in water (1×10^{-3} M^{-1}, concentration of dopant for **P-300**, Table 1) indicate that more than 99.4% of the azobenzene-sulfonic acid molecule exists in the form of the micelles in water and their average diameters were obtained as 4.29 nm. The

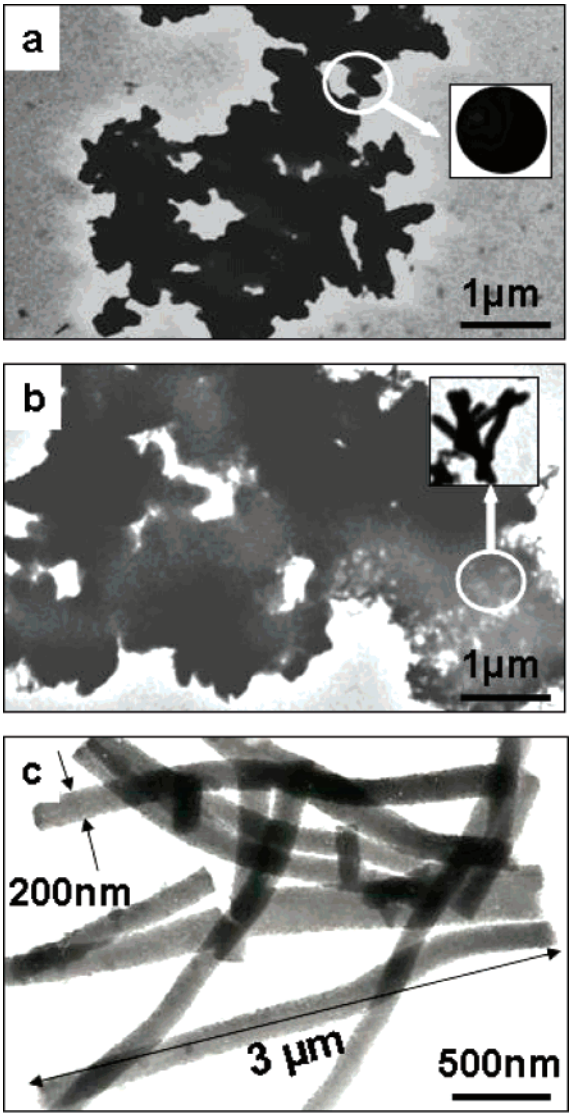

Figure 4. TEM images of polyaniline materials: (a) **P-I-300**, (b) **P-I-450**, and (c) **P-E-300**.

theoretical geometry of the dopant molecule was calculated using AM1 calculations (see Figure 5) and found that the end-to-end distance of the polar head to hydrophobic tail was obtained as 24.4 Å (or 2.44 nm). The diameter of the tightly packed spherical micelle is expected to be equal to the double length of the end-to-end distance of the molecule. It was calculated as 2×2.44 nm $= 4.88$ nm, which is almost matching with that of the value obtained experimentally by DLS. It confirms that the new renewable resource based azobenzenesulfonic acid derivatives are good surfactants and form stable spherical micelles in water (more than 99%). DLS measurements were also performed for solution containing APS + dopant and aniline + dopant and the data are shown in Figure 5. Upon adding APS to the dopant micelles in water, the solution slowly becames turbid. DLS data of the turbid solution indicate the presence of two types of distribution with aggregates in 2.13 and 5.29 μM range (see Figure 5). The turbid solution was stable for more than 24 h at room temperature and slowly red solid start to precipitate from the solution after 1 day. The UV−vis spectrum of the isolated red precipitate is almost identical to that of the original azobenzene chromophores (see Supporting Information), which ruled out the possibility of any oxidation between APS and dopant. It confirms that upon adding APS to dopant in water larger aggregates of 2−5 μM in size were produced which are stable and dispersed in the aqueous phase for more than 24 h. The addition of aniline to dopant produces pale yellow thick emulsion and DLS data of the resultant emulsion showed predominately aggregates in 5.13 μm with small amount in 2.32 μM. The emulsion was stable up to more than 10 days at room temperature and no precipitate or isolation of layers were noticed. The above DLS experiments clearly indicate that amphiphilic molecule has tendency to form stable aggregates with both APS and aniline in water under the polymerization conditions.

In the present investigation, two kinds of aggregations are possible in the interfacial polymerization: (i) formation of pre-aggregated templates in the aqueous layer between APS + amphiphilic dopant and (ii) the aniline + amphiphilic dopant micellar templates at the interface. An independent control experiment was carried out by taking aniline in the organic layer and dopant in aqueous layer (without APS) to check the formation of turbid emulsion at the interface. Surprisingly, the diffusion of aniline to aqueous layer did not produce any turbid layer at the interface for more than 24 h (see Supporting Information). It ruled out the possibility of aniline + dopant complex templating the interfacial polymerization. Therefore, it can be assumed that the APS + dopant pre-aggregates in the aqueous phase control the shape and size of the polyaniline nanomaterials. On the basis of the DLS measurements and control experiment, the mechanism for the selective aggregation of dopant in both interfacial and emulsion route is described in Figure 6. The individual micelles in complexation with aniline or ammonium persulfate produce large micrometer size aggregated micelles which behave as templates for the nanomaterial synthesis. The amphiphilic azobenzenesulfonic acid exists in the form of 4.3 nm micelles in water and undergoes aggregation in the presence of APS and aniline in water to produce larger aggregates of 2 to 5 μM in range. In the interfacial route, the diffusion of aniline from the organic phase get absorbed at the surfaces of the APS + dopant spherical aggregates and subsequently get oxidized to produce polyaniline nanospheres. On the other hand, in the emulsion route, the aniline + dopant complex exists in the form of cylindrical micelles and addition of APS subsequently oxidizes the matrix to form polyaniline nanofibers. The SEM pictures (Figures 2 and 3) indicate that the morphology of the materials in the interfacial route was more sensitive to the aniline/dopant ratio in feed compared to emulsion route. The samples **P-I-100** and **P-I-300** were predominantly spheres, however, the decreasing the amount of dopant changes the morphology from spheres to fibers in **P-I-450**. To confirm the above morphological changes, the particle size distribution of polyaniline spheres were determined by static light scattering technique and shown in Figure 7. **P-I-100** showed broad distributions with three peak maxima at 200, 400, and 1300 nm. It indicates that that the sample contains a mixture of nano and micro spheres, which is further evident from its SEM images (Figure 2a). **P-I-300** showed two types of distributions with predominantly particles in 400 nm with a small amount in 130 nm sizes. It suggests that majority of the polyaniline spheres in **P-I-300** have a diameter of 400 nm and this value is in good agreement with that of SEM and TEM analysis (Figure 2b and Figure 4a). The sample **P-I-450** did not pass the particle size measurement which may be due to the presence of fibrous properties of the sample as evident from the SEM and TEM images (see Figure 2c and 4b). The particle size distribution in Figure 7 is a result of the variation in the template formation of dopant with APS in the interfacial route in water. The broad tri-model particle distribu-

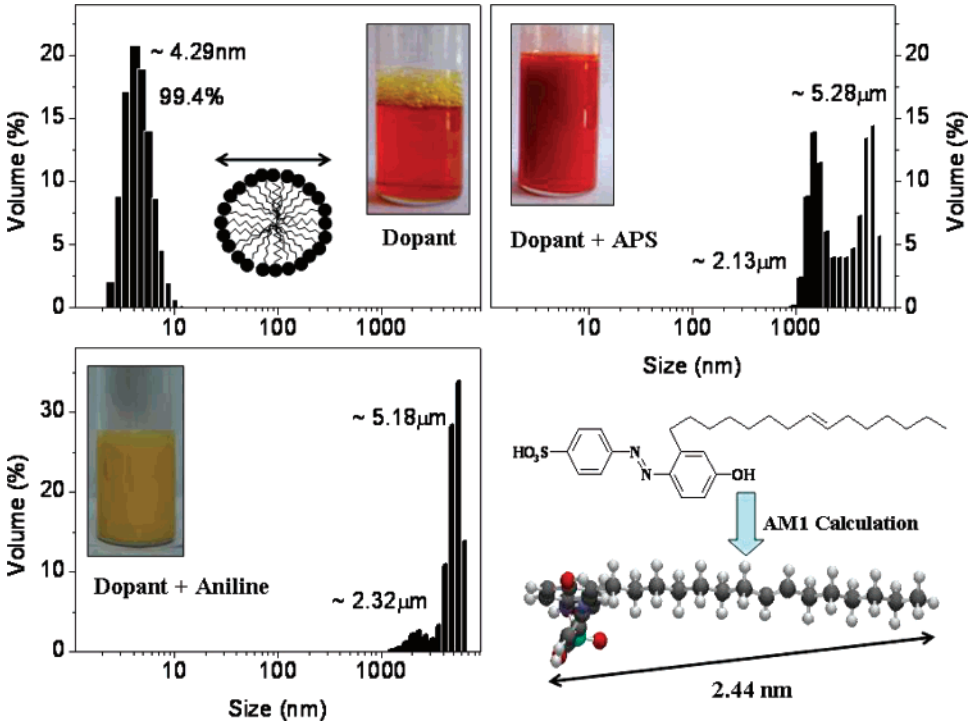

Figure 5. DLS measurements of dopant, dopant + aniline and dopant + APS complexes. The theoretical geometry of the dopant was calculated using AM1 model.

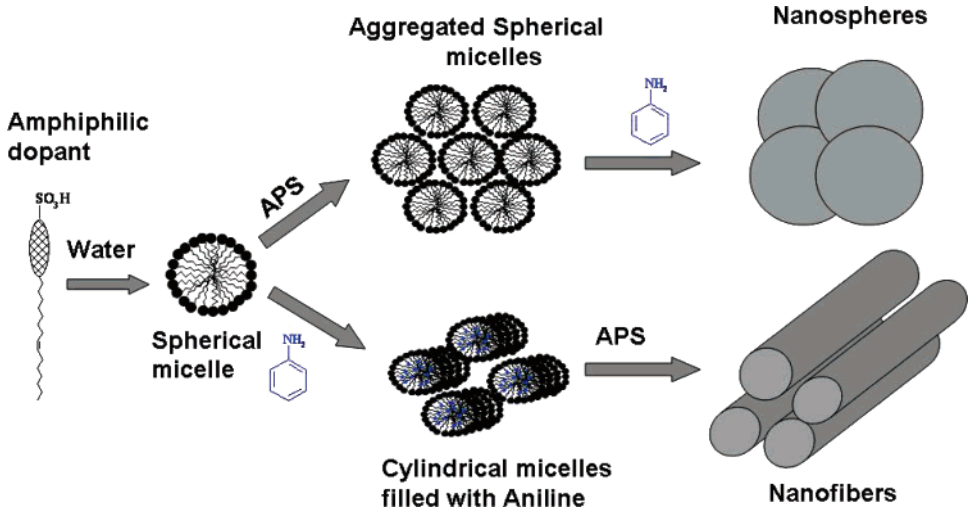

Figure 6. Possible mechanism for the formation of polyaniline nanomaterials based on a single molecular dopant approach via interfacial (top) and emulsion (bottom) routes.

tion in **P-I-100** indicates the existence of APS + dopant spherical aggregates in various sizes in the aqueous layer. The dilution of dopant amount in aqueous layer results in the formation of homogeneous aggregates, which produces more uniform nanospheres in **P-I-300**. Further dilution of dopant in the APS + dopant mixture in the aqueous layer; disturb the aggregate formation and results in the formation of fiber plus spheres in **P-I-450**. These intermediate states are only stable in the aqueous medium and the isolation and characterization of size and the shape of the aggregates were very difficult. However, the tracing of the intermediate aggregates by techniques such as cryo-TEM may be very useful, which will be addressed in elsewhere. Nevertheless, in the present investigation, the DLS data adequately support the existence of the various possible aggregates (as shown in Figure 6) and the morphologies of the resultant polyaniline nanomaterials (SEM and TEM images) further support the mechanistic pathways.

The polyaniline nanomaterials were freely suspendable in water and other organic solvents by simple mixing under ultrasonic stirring at room temperature. UV−vis spectra of dopant and nanomaterial samples are recorded in water are shown in Figure 8. The absorbance spectrum of dopant **1** has three characteristic peaks at 245, 360, and 460 nm corresponding to $\pi-\pi^*$ (cis), $\pi-\pi^*$(trans), and n$-\pi^*$ (cis), respectively.[34] It is clear from the figure that the absorption spectra of polyaniline nanomaterials are free from quinoid ring (at 650 nm), which confirm the efficient doping of dopant. The peak at 450 and broad peak (or tail) above 800 nm are corresponding to polaron or bipolaron n$-\pi^*$ transitions of the polyaniline, respectively.[38] The near-IR region of absorption spectra of polyaniline nanospheres and nanofibers were completely different (above 850 nm). MacDiarmid and co-workers studied the secondary doping of simple polyaniline−CSA-doped materials (not nanomaterials) by *m*-cresol solvent.[39,40] They reported that the more coil-like

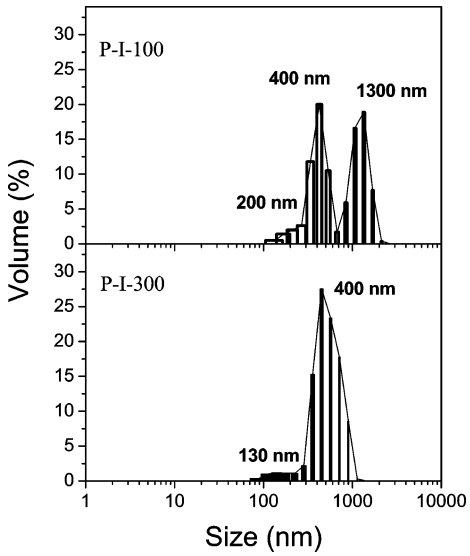

Figure 7. Particle size distribution of nanospheres prepared via interfacial route.

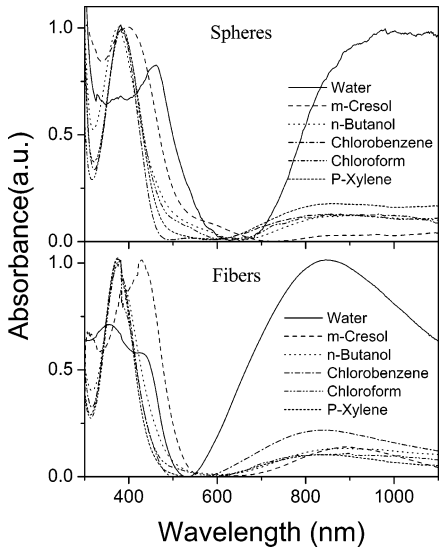

Figure 9. UV−vis spectra of polyaniline nanomaterials in various solvents at 30 °C.

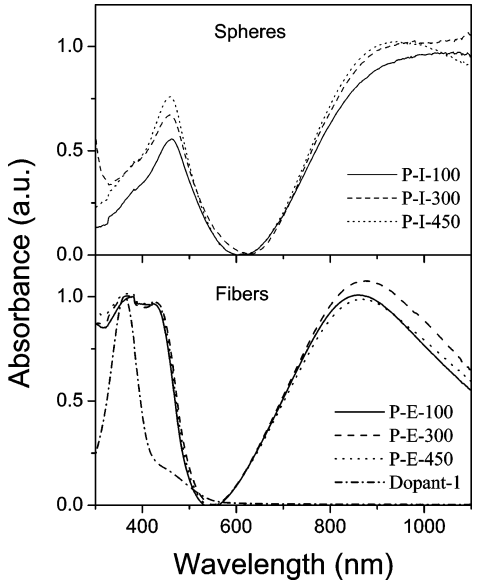

Figure 8. UV−vis spectra of dopant and polyaniline nanomaterials in water at 30 °C.

confirmation in polyaniline chains have a peak characteristic at 800 nm whereas expanded chain conformation showed a free carrier tail commencing at 950−1000 nm in the near IR-region. Recently, Li et al. reported the observation of expanded chain conformation in polyaniline nanofibers during the course of interfacial polymerization using UV−vis spectroscopy for HCl dopant in xylene/water bilayer system.[41] Interestingly, in the present case, the absorbance spectra of the nanospheres (not nanofibers) showed a free carrier tail above 950 nm indicating the delocalization of electrons in the polaron band for the expanded conformation of polyaniline chains. On the other hand, the polyaniline nanofibers produce by the same amphiphilic dopant via emulsion route showed a peak characteristic at 830 nm corresponding to the more coiled-like conformation. It is important to note that the presence of spheres plus fibers in **P-I-450** (see Figures 2 and 4) partially disturb the expanded conformation of the polymer chains, which is further reflected on the absorbance spectra. The samples **P-I-100** and **P-I-300** (see Figures 2 and 4) predominantly have only nanospheres and their absorbance spectra confirmed that they are in expanded polymer chain confirmation. The interfacial polymerization is mainly driven by the selective solubility of the polymer chains specifically in one of the solvent medium at the interface for driving the equilibrium to form of higher molecular weight chains. In the present interfacial polymerization route, the resultant hydrophilic (also charged) polyaniline emeraldine salt has more affinity toward water rather than the organic phase. The higher water affinity of the charged chains drive the polymerization equilibrium for the formation of higher molecular weight chains by dissolving itself in the aqueous phase and create more active site at the interface for further growth. In general, polymer chains have more tendencies for expanded conformation in solvents compared to their solid state. Therefore, during the polymerization, the soluble polymer chains adopt expanded confirmation in the aqueous layer, which act as a nucleating site for subsequent growth of expanded polyaniline nanospheres. On the other hand, in the emulsion route, such a solvent-driven uni-directional growth is not possible, and therefore, the nanofibers were obtained in a more coiled-like conformation compared to that of the interfacial route.

The presence of hydrophobic tail in the amphiphilic dopant increases the solubility of both polyaniline nanospheres and fibers in common organic solvents. The materials can be easily suspended in chloroform, *n*-butanol, chlorobenzene, xylene, and *m*-cresol, etc, which is rarely reported for polyaniline nanomaterials. To study the effect of solvents on the expanded chain to coil-like conformation, the UV−vis spectra of the **P-I-300** (spheres) and **P-E-300** (fibers) were recorded in various solvents and shown in Figure 9. It is clear from the spectra that optical density of the bipolar transition is affected by the organic solvents, however, the conformations of the polymer nanomaterials are retained and less influenced by the solvent in which they were suspended. The absorption of polaron peaks at the lower wavelength region (∼400 nm) was blue-shifted for samples recorded in organic solvents compared to that of water (except *m*-cresol). The optical density of the absorption band corresponding to the delocalized bi-polaron of polyaniline nanofibers and spheres (above 950 nm) were more susceptible in organic solvents, however the chain conformations were not affected. It confirms that the conformations of the polymer chains in the nanomaterials are predominately controlled during the chemical polymerization techniques and not affected by the solvents in which they were dispersed. This observation is just opposite to MacDiarmid and co-workers[39] report of drastic

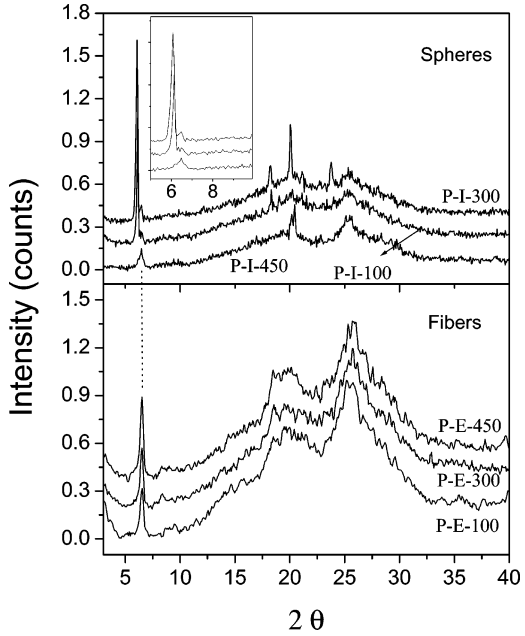

Figure 10. WXRD plots of polyaniline nanomaterials at 30 °C.

conformational changes in simple polyaniline emeraldine system (not polyaniline nanomaterials) due to the presence of *m*-cresol or chloroform. Since the conformation of polymer chains in polyaniline nanomaterials (both nanospheres and fibers) are almost unaltered by the various solvent, it can be assumed that once the polymer chains are confined to a particular topology at the nanometer level, they are less influenced by the external stimuli such as the solvent nature and its polarity. In the present case, a single molecular dopant approach was utilized to control the conformation of polyaniline chains in nanodomains via selectively self-organization in the interfacial and emulsion routes. Therefore, it may be assumed that the pre-templating behavior of the dopant complex and also the types of the polymerization routes determine the conformation of polyaniline nanomaterials. More detailed studies on solvent and temperature-dependent photophysical experiments to investigate the conformation of the polyaniline nanomaterials are currently in progress (these will be published latter). The four probe conductivity of nanospheres **P-I-100**, **P-I-300**, and **P-I-450** were obtained in the range of $\sim 10^{-2}$ S/cm, which is one ordered higher than that of nanofibers **P-E-100, P-E-300**, and **P-E-450** ($\sim 10^{-3}$ S/cm) (see Table 1). The conductivity of the polyaniline nanomaterials matched with that of the reported values.[34,45,46] It suggest that the expanded confirmation of polyaniline chains in spheres increase the delocalization of charge carriers (evident by UV−vis spectra; see Figure 8) and produced conductivity one order higher than that of nanofibers. Since the degree of doping (*S*/*N* ratio see Table 1) in both fibers and spheres are comparable, we can conclude that the more expanded confirmation chains increase the electrical conductivity of the polyaniline nanomaterials.

To further confirm the conformational changes in the polyaniline chains (nanofibers and spheres) and also to study the solid state behavior of the dopant molecule with polyaniline nanomaterials, finely powdered samples were subjected to wide-angle X-ray diffraction analysis at 30 °C. In the presence of functional dopants, the dopant−polymer undergoes various interactions, which tend to organize the polymer chains in three-dimensional highly ordered fashions. WXRD spectra for interfacial and emulsion route samples are given in Figure 10 and 2θ and *d*-spacing values are given in Table 1. The WXRD patterns of nanofibers (**P-E-100, P-E-300**, and **P-E-450**) showed three distinct peaks at $2\theta = 6.4$, 20.1, and 25.5° (*d*-spacing = 13.6, 4.4, and 3.5 Å, respectively). The two peaks at 20.1 and 25.5° are generally observed in doped polyaniline, but the peak at $2\theta = 6.4°$ is only observed for highly ordered samples in which the polyaniline chain distance increased by effective interdigitations of dopant molecules.[41−43] The increase in the peak intensity at $2\theta = 6.4°$ revealed the enhancement of solid state ordering of nanofibers by reducing the amount of dopant in the feed, which is in accordance with our earlier report.[33,34] The WXRD patterns of nanospheres were different from that of nanofibers. In the case of **P-I-100** and **P-I-300**, a new intense peak at $2\theta = 6.05°$ (*d*-spacing 14.3 Å) is observed in addition to a peak at $2\theta = 6.4°$ (*d*-spacing 13.6 Å, as observed in fibers). The presence of a new intense peak at $2\theta = 6.05°$ is indicating that the polymer chains in nanospheres possess more expanded chain conformation for increased solid state ordering compared to that of the nanofibers. The lower angle peak at $2\theta = 6.05°$ is more intense for uniformly distributed nanospheres **P-I-300** compared to broadly distributed sample **P-I-100** (see Figure 7). **P-I-450** has mixture of nanospheres + fibers, and therefore, the expanded conformation of polymer chains were disturbed, which accounts for the vanishing of the low angle peak at $2\theta = 6.05°$. The X-ray diffraction data supports the expanded chain conformation in polyaniline nanospheres compared to that of the polyaniline nanofibers.

Conclusion

We have shown that the shape, size and conformation from expanded chain to coil-like form of polyaniline nanomaterials can be controlled by selectively templating a new renewable resource based amphiphilic azobenzenesulfonic acid dopant in interfacial and emulsion polymerization routes. The amphiphilic molecule is efficient structure directing dopant for polyaniline nanomaterials and the approach demonstrated here have many unique features and advantages: (i) the amphiphilic azobenzenesulfonic acid molecule exist in the form of ~ 4.3 nm spherical micelles in water for templating polyaniline nanomaterials. (ii) The dopant micelles form spherical aggregates with APS in the aqueous layer and the diffusion of aniline (in the interfacial layer) into these spherical aggregates get oxidized to produce polyaniline spheres of 200−400 nm. (iii) The complexation of amphiphilic micelles with aniline produces stable milky cylindrical shaped aggregated micelles (in the emulsion routes), which upon oxidation by APS produces nanofibers of 200 nm diameter with length of 3−8 μM. (iv) both interfacial and emulsion routes were investigated for a wide range of composition of aniline/dopant ranging from 100 to 450 (in moles). (v) DLS and particle size analyzer were utilized to trace the mechanistic aspects of the polyaniline nanomaterials formation. (vi) The absorbance spectra indicate the formation of "expanded conformation" of polyaniline chains in the nanospheres produced via interfacial route. The nanofibers produced via emulsion route were much less ordered and the polyaniline chain found in the form of more coiled-like conformation. (vii) WXRD data confirmed the presence of expanded conformation in nanospheres and a new peak is observed at $2\theta = 6.05°$ (*d*-spacing 14.3 Å), which is absent in the nanofibers. The polyaniline nanomaterials are freely soluble in water and various organic solvents which are added advantages to process them for applications in opto-electronics and also to study the polyaniline aggregation properties by spectroscopic techniques. In the present investigation, we have used a new renewable resource based amphiphilic azobenzenesulfonic acid as a dopant to control the shape, size, solid state ordering, conductivity, and

conformation of polyaniline nanomaterials via interfacial and emulsion polymerization techniques.

Acknowledgment. We thank Department of Science and Technology, New Delhi, India under Schemes: DST/TSG/ME/2005/33 and NSTI Programme-SR/S5/NM-06/2007; KSCTSE, Thiruvananthapuram, Kerala, India (082/SRSPS/2004/CSTE) for financial support. The authors thank Dr. Peter Koshy, Mr. M. R. Chandran, Dr. U. Syamaprasad, and Mr. P. Gurusamy, RRL-Trivandrum for SEM and WXRD analysis. We also thank Dr Annie John and Mr.Willy Paul, SCTIMST, Trivandrum for TEM and dynamic light scattering analysis. P. Anilkumar thanks UGC−New Delhi, India for junior research fellowship.

Supporting Information Available: Text giving additional information for synthesis and characterization of the dopant, and figures showing FT-IR spectra of the nanomaterials, the photographs of dopant-aniline emulsion, a snapshot showing interfacial polymerization of aniline, UV−vis spectra of dopant and dopant-APS complex, and TGA plots of nanomaterials. This material is available free of charge via the Internet at http://pubs.acs.org.

References and Notes

(1) Janata, J.; Josowicz, M. *Nat. Mater.* **2002**, *2*, 19−24.
(2) Virji, S.; Fowler, J. D.; Baker, C. O.; Haung, J.; Kaner, R. B.; Weiller, B. H. *Small* **2005**, *1*, 624−627.
(3) Virji, S.; Kaner, R. B.; Weiller, B. H. *J. Phys. Chem. B* **2006**, *110*, 22266−22270.
(4) Virji, S.; Haung, J.; Kaner, R. B.; Weiller, B. H. *Nano. Lett.* **2004**, *4*, 491−496.
(5) Haung, J.; Virji, S.; Weiller, B. H.; Kaner, R. B. *Chem.—Eur. J.* **2004**, *10*, 1314−1319.
(6) Liu, J.; Lin, Y.; Liang, L.; Voigt, J. A.; Huber, D. L.; Tian, Z. R.; Coker, E.; Mckenzie, B.; Mcdermott, M. J. *Chem.—Eur. J.* **2003**, *9*, 604.
(7) Sukeerthi, S.; Contractor, A. Q. *Anal. Chem.* **1999**, *71*, 2231−2236.
(8) Feng, X.; mao, C.; Yang, G.; Hou, W.; Zhu, J. J. *Langmuir* **2006**, *22*, 4384−4389.
(9) Ma, Y.; Ali, S. R.; Dodoo, A. S.; He, H. *J. Phys. Chem. B* **2006**, *110*, 16359−16365.
(10) Zhang, X.; Goux, J. W.; Manohar, S. K. *J. Am. Chem. Soc.* **2004**, *126*, 4502−4503.
(11) Alam, M. M.; Wang, J.; Guo, Y.; Lee, S. P.; Tseng, H. R. *J. Phys. Chem. B.* **2005**, *109*, 12777−12784.
(12) Tseng, R. J.; Haung, J.; Ouyang, J.; Kaner, R. B.; Yang, Y. *Nano. Lett.* **2005**, *5*, 1077−1080.
(13) Wang, J.; Chan, S.; Carlsoin, R. R.; Luo, Y.; Ge, G.; Ries, R. S.; Heath, J. R.; Tseng, H. R. *Nano Lett.* **2004**, *4*, 1693−1697.
(14) Parthasarathy, R. V.; Martin, C. R. *Chem. Mater.* **1994**, *6*, 1627−1632.
(15) Qiu, H.; Zhai, J.; Li, S.; Jiang, L.; Wan, M. *Adv. Funct. Mater.* **2003**, *13*, 925−928.
(16) Qiu, H.; Wan, M.; Matthews, B.; Dai, L. *Macromolecules* **2001**, *34*, 675−677.
(17) Meng, L.; Lu, Y.; Wang, X.; Zhang, J.; Duan, Y.; Li, C. *Macromolecules* **2007**, *40*, 2981−2983.
(18) Wei, Z.; Zhnag, Z.; Wan, M. *Langmuir* **2002**, *18*, 917−921.
(19) Li, C.; Hatano, T.; Takeuchi, M.; Shinkai, S. *Chem. Commun.* **2004**, 2350−2351.
(20) Haung, J.; Virji, S.; Weiller, B. H.; Kaner, R. B. *J. Am. Chem. Soc.* **2003**, *125*, 314.
(21) Haung, J.; Kaner, R. B. *J. Am. Chem. Soc.* **2004**, *126*, 851−855.
(22) Sawall, D. D.; Villahermosa, R. M.; Lipeles, R. A.; Hopkins, A. R. *Chem. Mater.* **2004**, *16*, 1606−1608.
(23) Haung, J.; kaner, R. B. *Chem. Commun.* **2006**, 367−376.
(24) Haung, J.; Kaner, R. B. *Angew. Chem.* **2004**, *116*, 5941−5945.
(25) Wang, J.; Bunimovich, L. Y.; Sui, G.; Savvas, S.; Wang, J.; Guo, Y.; Heath, J. R.; Tseng, H. R. *Chem. Commun.* **2006**, 3075−77.
(26) Li, W.; Wang, H. L. *J. Am. Chem. Soc.* **2004**, *126*, 2278−2279.
(27) Chiou, N. R.; Epstein, A. J. *Adv. Mater.* **2005**, *17*, 1679−1683.
(28) Haung, K.; Wan, M. X. *Chem. Mater.* **2002**, *14*, 3486−3492.
(29) Zhang, L.; Wan, M. X. *Adv. Funct. Mater.* **2003**, *13*, 815−820.
(30) Li, G.; Zhang, Z. *Macromolecules* **2004**, *37*, 2683−2685.
(31) Zhnag, Z.; Wei, Z.; Wan, M. *Macromolecules* **2002**, *35*, 5937−5942.
(32) Carswell, A. D. W.; O'Rear, E. A. O.; Grady, B. P. *J. Am. Chem. Soc.* **2003**, *125*, 14793.
(33) Anilkumar, P.; Jayakannan, M. *Langmuir* **2006**, *22*, 5952−5957.
(34) Anilkumar, P.; Jayakannan, M. *J. Phys. Chem. C* **2007**, *111*, 3591−3600.
(35) Santos, M. L.; Magabhaes, G. C. *J. Braz. Chem. Soc.* **1999**, *10*, 13−20.
(36) Hassan, P. A.; Sawant, S. N.; Bagkar, N. C.; Yakhmi, J. V. *Langmuir* **2004**, *20*, 4874−4880.
(37) Hassan, P. A.; Raghavan, S. R.; Kaler, E. W. *Langmuir* **2002**, *18*, 2543−2548.
(38) Li, X. G.; Lu, Q. F.; Huang, M. R. *Chem.—Eur. J.* **2006**, *12*, 1349−1359.
(39) MacDiarmid, A. G.; Epstein, A. J. *Synth. Met.* **1995**, *69*, 85−92.
(40) Min, Y.; Xia, Y.; MacDiarmid, A. G.; Epstein, A. J. *Synth. Met.* **1995**, *69*, 159−160.
(41) Li, W.; Zhu, M.; Zhang, Q.; Chen, D. *Appl. Phys. Lett.* **2006**, *89*, 103110.
(42) Lunzy, W.; Banka, E. *Macromolecules* **2000**, *33*, 425.
(43) Jayakannan, M.; Annu, S.; Ramalekshmi, S. *J. Polym. Sci., Polym. Phys.* **2005**, *43*, 1321−1331.
(44) Jana, T.; Nandi, A. K. *Langmuir* **2000**, *16*, 3141.
(45) Wei, Z.; Wan, M. *Adv. Mater.* **2002**, *14*, 1314−1317.
(46) Zhang, L.; Wan, M.; Wei, Y. *Macromol. Rapid Commun.* **2006**, *27*, 888−893.

MA071292S